

Development of a simple CT scanner for a cultural property

Prof. Mitsuyoshi Kureya
Gunma College of Technology
580 Toriba-Machi, Maebashi, Gunma 371
Japan
V.

1. Introduction

So far, the internal structure of wooden statue has been investigated by Analytical X-ray Photogrammetry. But the tomography of the internal structures of wooden statues, especially the apparatus for this purpose, is an untouched field (Refer to Fig.1)

Sometimes medical CT scanners are used for the study of cultural property. But the above procedure has some difficulties, since the transportation of an old wooden statue and setting of the statue on to a CT scanner is rather difficult.

Since it is difficult to move CT scanners from hospitals and they are expensive, a simple low-cost and portable CT scanner must be developed.

Fig.1-1 is the object : Wooden statue " JUNI-SHINZO"
Fig.1-2 is the object with control points.
Fig.1-3 is an X-ray photograph.
Fig.1-4 is the measured result.



Fig.1-1.

Object. JUNI SHINZO



Fig.1-2.

Object with control-point.



Fig. 1-3.
Object-photograph X-ray.

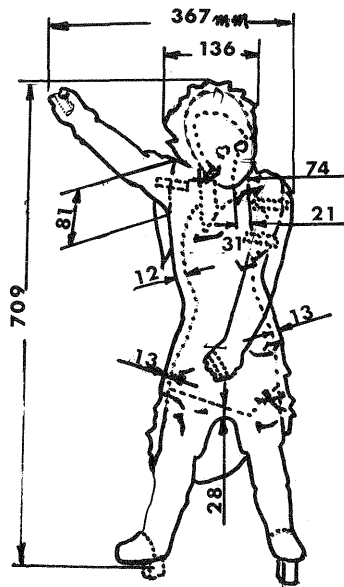


Fig. 1-4.
Result.

2. Basic theory of Tomogram

Although the basic theory of tomogram is well known, the outline of it and some important points shall be described as follows.

2-1. Absorption coefficient

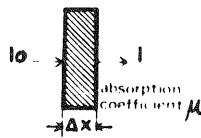


Fig. 2-1

X-ray which the intensity I_0 was radiated on the material which had the thickness of Δx and the absorption coefficient μ as shown in Fig. 2-1.

$$I = I_0 e^{-\mu \Delta x} \quad (2-1)$$

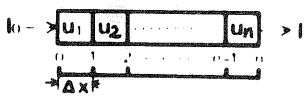


Fig. 2-2

the equation (2-1) is also written as

$$\mu \Delta x = \ln \frac{I_0}{I} \quad (2-2)$$

Now the μ and Δx are described in the one dimensional discrete model as in Fig. 2-2.

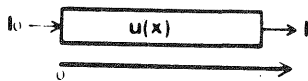


Fig. 2-3

$$\ln \frac{I_0}{I} = \sum_{i=1}^n \mu_i \Delta x \quad (2-3)$$

Fig. 2-1, 2-2, 2-3.

in the one dimensional continuous model as in Fig. 2-3, the equation is

$$\ln \frac{I_0}{I} = \int_0^l \mu(x) dx \quad (2-4)$$

2-2. Projected data

As shown in Fig.2-4, the object has the absorption coefficient of X-ray with the distribution described by $f(x,y)$ in the X-Y coordinates. The X-Y coordinates is inclined by the angle of θ .

Now the X-ray with the intensity of I_0 is radiated from the X-ray tube parallel to Y-axis. the X-ray passes through the object $f(x,y)$ as it is decreased and its intensity is measured by the detector. If the intensity is I , the equation from the one dimensional continuous model is described as

$$\ln \frac{I_0}{I} = \int_{-\infty}^{\infty} f(x,y) dY \quad \text{-----} \quad (2-5)$$

Now the X-ray tube and the detector is moved in the direction of X-coordinate and the intensity of X-ray is measured by the detector. The rate of decrease $\ln(I_0/I)$ is shown in Fig.2-4 (b) and is called projected data. The projected data is the function of X, the parallele-moved distance of X-Ray tube, and the angle θ . Thus, the projected data is described by $g(X, \theta)$. From the transformation of the X-Y coordinates and x,y ,

$$\begin{aligned} x &= X \cos \theta - Y \sin \theta \\ y &= X \sin \theta + Y \cos \theta \end{aligned} \quad \text{-----} \quad (2-6)$$

the projected data $g(X, \theta)$ is described by the equation (2-5) as

$$g(X, \theta) = \int_{-\infty}^{\infty} f(X \cos \theta - Y \sin \theta, X \sin \theta + Y \cos \theta) dY \quad \text{-----} \quad (2-7)$$

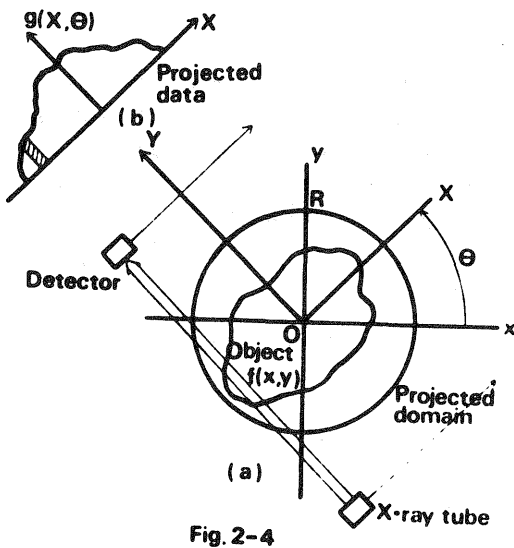


Fig.2-4.

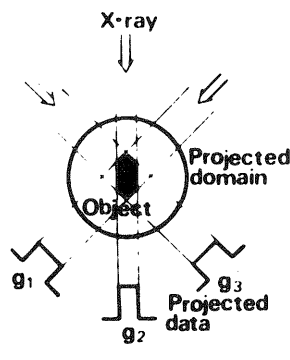


Fig.2-5.

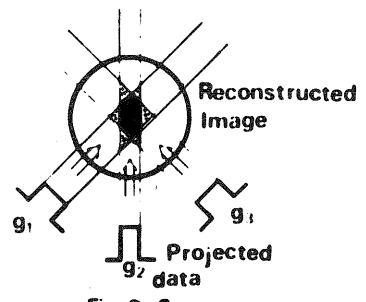


Fig.2-6.

2-3. Reconstruction method

The filtered back projection FBP is used as reconstruction method. To have some understanding, the back projection method is described in 2-3-1 and Fourier transformation is described for

the theoretical ground . In 2-3-3, the filtered back projection method is explained.

2-3-1. Back projection

The back projection described here is the simplest reconstruction method to gain the distribution of the absorption coefficient from the projected data. The projected data g_1, g_2, g_3 obtained as in Fig.2-5 are simply projected back together to conceive a reconstructed image . Although the basic theory of the method is intuitively clear , it is also speculated that the image is blurred. Thus, the back projection method is not used in CT.

The image $b(x,y)$ obtained by back projection is;

$$b(x,y) = \int_0^\pi g(X, \theta) d\theta \quad \text{----- (2-8)}$$

2-3-2. Fourier transformation

The distribution of the absorption coefficient can be obtained from the projected data by this Fourier transformation. The two dimensional Fourier transformation $F(\xi, \eta)$ of the distribution of the absorption coefficient is ;

$$F(\xi, \eta) = \int_{-\infty}^{\infty} \int_{-\infty}^{\infty} f(x,y) \exp \{-j2\pi(\xi x + \eta y)\} dx dy \text{----- (2-9)}$$

If $F(\xi, \eta)$ is obtained by some way from the projected data, the required distribution $f(x,y)$ of the absorption coefficient is as follows.

$F(\xi, \eta)$ expressed by orthogonal coordinates is transformed into polar coordinates as in Fig.2-7.

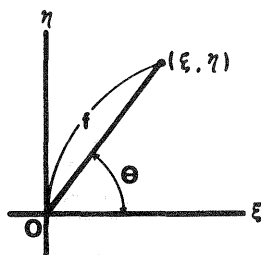


Fig. 2-7

Fig.2-7.

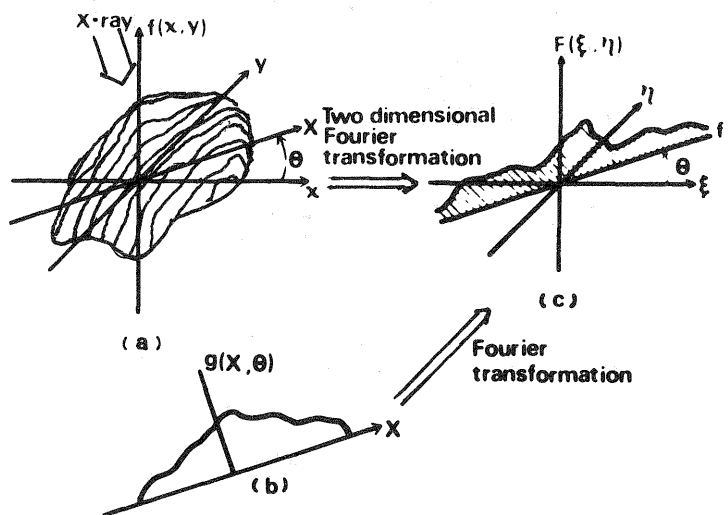


Fig.2-8

Fig.2-8.

The transformation equation is;

$$\begin{aligned} \xi &= f \cos \theta \\ \eta &= f \sin \theta \end{aligned} \quad \text{----- (2-10)}$$

Therefore, $F(\xi, \eta)$ is;

$$F(f \cdot \cos \theta, f \cdot \sin \theta) = \int_{-\infty}^{\infty} \int_{-\infty}^{\infty} f(x, y) \exp \{ -j2\pi f(x \cdot \cos \theta - y \cdot \sin \theta) \} dx dy \quad \text{-----} \quad (2-11)$$

From the equation (2-6),

$$F(f \cdot \cos \theta, f \cdot \sin \theta) = \int_{-\infty}^{\infty} \int_{-\infty}^{\infty} f(X \cdot \cos \theta - Y \cdot \sin \theta, X \cdot \sin \theta + Y \cdot \cos \theta) \cdot \exp(-j2\pi fX) dXdY = \int_{-\infty}^{\infty} \left(\int_{-\infty}^{\infty} f(X \cdot \cos \theta - Y \cdot \sin \theta, X \cdot \sin \theta + Y \cdot \cos \theta) dY \right) \exp(-j2\pi f \cdot X) dX$$

The integral in the brackets is noticed to be the same as the definition of the projected data (2-7).

Thus,

$$F(f \cdot \cos \theta, f \cdot \sin \theta) = \int_{-\infty}^{\infty} g(X, \theta) \exp(-j2\pi fX) dX \quad \text{-----} \quad (2-12)$$

Therefore, $F(f \cdot \cos \theta, f \cdot \sin \theta)$ which is the two dimensional Fourier transformation of the distribution of the absorption coefficient, $f(x,y)$, can be obtained by the Fourier transformation of the projected data $g(X, \theta)$.

The distribution of the absorption coefficient $f(x,y)$ is as follows.

$$f(x,y) = \int_{-\infty}^{\infty} \int_{-\infty}^{\infty} F(\xi, \eta) \exp(j2\pi(\xi x + \eta y)) d\xi d\eta \quad \text{-----} \quad (2-13)$$

The above method is summarized in Fig.2-8. Suppose Fig.2-8 (a) is the distribution of the absorption coefficient $f(x,y)$. Fig.2-8 (c) is $f(x,y)$ after the two dimensional Fourier transformation. In Fig.2-8 (a), the two x-y coordinate systems

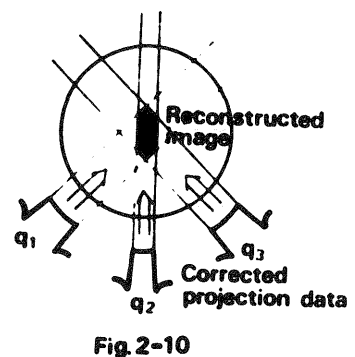
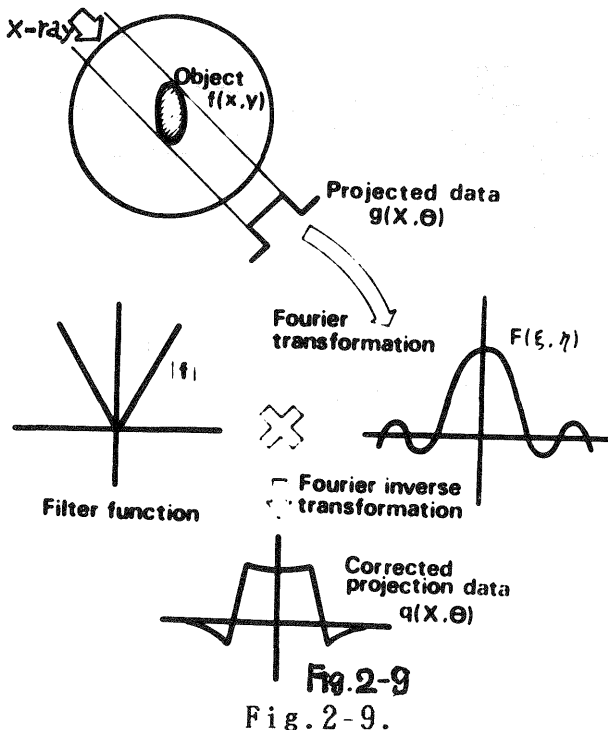


Fig.2-10.

with one of them angled at θ against the other is thought and X-ray is radiated parallel to the Y-coordinate. The projected data obtained thus is $g(X, \theta)$ in Fig.2-8(b). $g(X, \theta)$ after Fourier transformation is the cross section of $F(\xi, \eta)$ at the angle θ in Fig.2-8(c). Since the angle θ varies from 0 to π , $F(\xi, \eta)$ is obtained completely from the projected data $g(X, \theta)$ and by the two dimensional Fourier inverse transformation, the distribution of the absorption coefficient $f(x, y)$ is obtained.

2-3-3. Filtered back projection: FBP

The solution gained by the filtered back projection method is mathematically equivalent to that obtained by the above mentioned Fourier transformation. The distribution of the absorption coefficient $f(x, y)$ obtained by the Fourier transformation is following as mentioned before.

$$f(x, y) = \int_{-\infty}^{\infty} \int_{-\infty}^{\infty} F(\xi, \eta) \exp \{j2\pi(\xi x + \eta y)\} d\xi d\eta$$

The above is expressed in the polar coordinates instead of the orthogonal coordinates.

$$\begin{aligned} f(x, y) &= \int_0^{2\pi} \int_0^{\infty} F(f \cdot \cos \theta, f \cdot \sin \theta) \exp \{j2\pi f(x \cdot \cos \theta \\ &\quad + y \cdot \sin \theta)\} f \cdot df \cdot d\theta \\ &= \int_0^{\pi} \left[\int_{-\infty}^{\infty} F(f \cdot \cos \theta, f \cdot \sin \theta) \exp(j2\pi f X) |f| \cdot df \right] d\theta \end{aligned} \quad \text{----- (2-14)}$$

Here, the integral in the brackets is the Fourier inverse transformation of the projected data in θ direction $g(X, \theta)$ after $g(X, \theta)$ is transformed by Fourier transformation $F(f \cos \theta, f \sin \theta)$ and the filter function $|f|$ where f is the frequency is taken into consideration.

The integral in the brackets is expressed by $q(X, \theta)$;

$$q(X, \theta) = \int_{-\infty}^{\infty} F(f \cos \theta, f \sin \theta) |f| \exp(j2\pi f X) df \quad \text{----- (2-15)}$$

$q(X, \theta)$ is called the corrected projection's data here.

Thus, the equation (2-14) is written as;

$$f(x, y) = \int_0^{\pi} q(X, \theta) d\theta \quad \text{----- (2-16)}$$

The equation (2-16) is nothing but the back projection of the corrected projection's data $q(X, \theta)$.

The corrected projection's data is obtained by using the filter function $|f|$ on the projected data $g(X, \theta)$ in a certain frequency domain. And by back projection of the corrected projection's data $q(X, \theta)$, the distribution of the absorption coefficient $f(x, y)$ can be obtained. The process above is summarized in Fig. 2-9.

The corrected projection's data obtained by the process is back projected as in Fig.2-10 to have the complete distribution of the absorption coefficient $f(x, y)$. The blur mentioned in section 2-3-1 is corrected by the negative part of the cor-

rected projection's data to produce a perfect reconstructed image.

2-4. Fan beam and Parallel beam

The projected data $g(X, \theta)$ explained in section 2-2 is on the premise that it is obtained by parallel beam. However, fan beam as in Fig.2-12 is generally used in CT because the exposure time is short and the movable part is small in fan beam. Therefore, the projected data obtained by fan beam must be transformed into the projected data obtained by parallel beam. When a certain fan beam is transformed into a parallel beam,

the resultant parallel beam must have the inclination and the distance from the rotational center equal to those of the fan beam. The angle θ and the distance X from the rotational center required for the transformation are obtained from the angle β at the time of photographing and the position of the detector (Fig.2-12). The procedure is as follows.

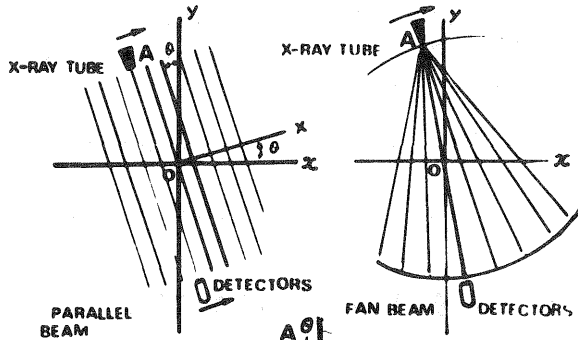


Fig.2-11

Fig.2-12

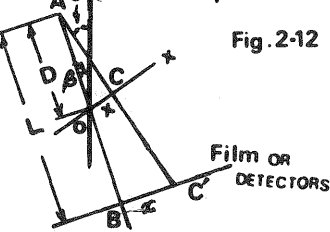


Fig.2-13

Fig.2-11, 2-12, 2-13. certain detector.

In Fig.2-13, $\triangle AOC$ and $\triangle AED$ are

$$D : X = \sqrt{L^2 + x^2} : x$$

$$\therefore X = \frac{D \cdot x}{\sqrt{L^2 + x^2}} \quad \text{----- (2-17)}$$

Here, $\angle OAC = \theta - \beta$

$$\sin(\theta - \beta) = \frac{x}{D}$$

$$\therefore \theta = \beta + \sin^{-1} \left(\frac{x}{D} \right) \quad \text{----- (2-18)}$$

3 . Outline and constitution of the system

Widely used CT scanners at present are mostly for medical pur-

poses and large in size. They are installed in hospitals and their transportation is impossible. Furthermore, the arms and legs of a statue or the accessories of it are not removable unlike those of a man (Fig.3-1). To economize cost, X-ray films are utilized in the experiment instead of the detector.

Fig.3-2 shows that it is a three component-system.

- (a) photographing.
- (b) collecting data.
- (c) information process.

3-1. Structure of the photographing instrument

The structure is shown in Fig.3-2 (a), and Lead (Pb) plate-screen having a slit (about 1 mm in width) is shown in Fig.3-3. An object is placed on a turn table at the front of the Lead plate screen. The movable cassette is set behind of the screen, and the cassette is moved in vertical direction along the spindle as shown in Fig.3-4. The turn table is set at the side of the X-ray tube, so the object is placed between the X-ray tube and the slit (namely the X-ray film).

3-1-1. Screen and Slit

The size of X-ray screen made of Lead (Pb) is 1200x700 mm.

On the screen plate, a slit (width 245 mm, gap-size of slit 1 mm above mentioned) is found horizontally.

The X-ray radiated from the source penetrates the object, passes the slit to reach the X-ray film. Therefore, the X-ray absorbed by the object gives the spectrum on the film comparable to the level of absorption. When one narrow spectrum is recorded on the film, the rotation table with the object rotates at the angle of $180^\circ/n$. n is designed to have values such as 64, 128, etc. calculated from $2^6=64$ or $2^7=128$. After the rotation, the film shifts on the screen plate 2 mm to 5mm in vertical direction. Here, X-ray is radiated on the object again. The series of process mentioned above is performed by remote control.

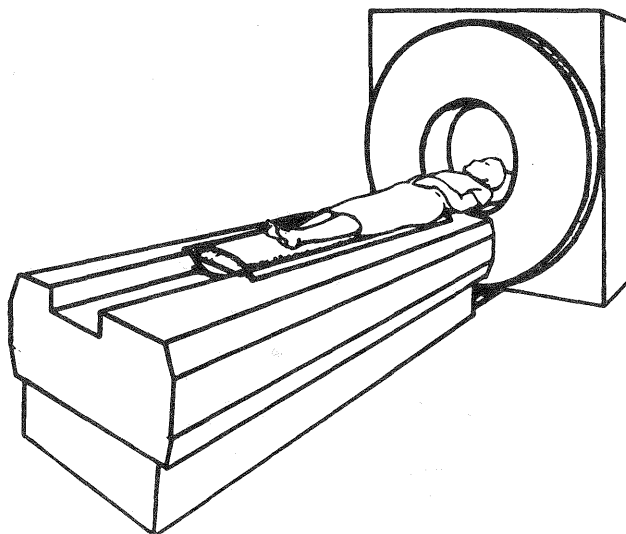


Fig.3-1

Fig.3-1

n is designed to have values such as 64, 128, etc. calculated from $2^6=64$ or $2^7=128$. After the rotation, the film shifts on the screen plate 2 mm to 5mm in vertical direction. Here, X-ray is radiated on the object again. The series of process mentioned above is performed by remote control.

3-1-2. Data collecting system

This part is shown in Fig. 3-2 (b) and is composed of a lamp, a condenser lens, a transparent glass plate movable in X and Y directions, an iris and a photomultiplier. n numbers of the band spectrums photographed and developed previously are placed on a glass plate to transform the spectrum data into electrical signals for output. The glass plate first moves in X direction as far as the length of the spectrum, stops and goes back to the

starting point. The glass plate now moves in Y direction for the next spectrum to repeat the same process until it finishes the nth spectrum. Fig.3-5 shows the photopattern analyzer and Fig.3-6 is the output from the photopattern analyzer.

3-1-3. Information process

The electrical signals from the data collecting system {refer to Fig.3-2(b), Fig.3-5, Fig.3-6 } are amplified appropriately and sent to a computer to be stored in a floppy disk.

If the satellite computer and a main computer are on line, the calculation for the reconstruction of an image is immediately proceeded to display the image on the screen. If on line system is not established, the floppy disk with the data may be brought to the main computer for reconstruction. The algorithms of fast Fourier transform constitute the image reconstruction program {refer to Fig.3-2 (c)}

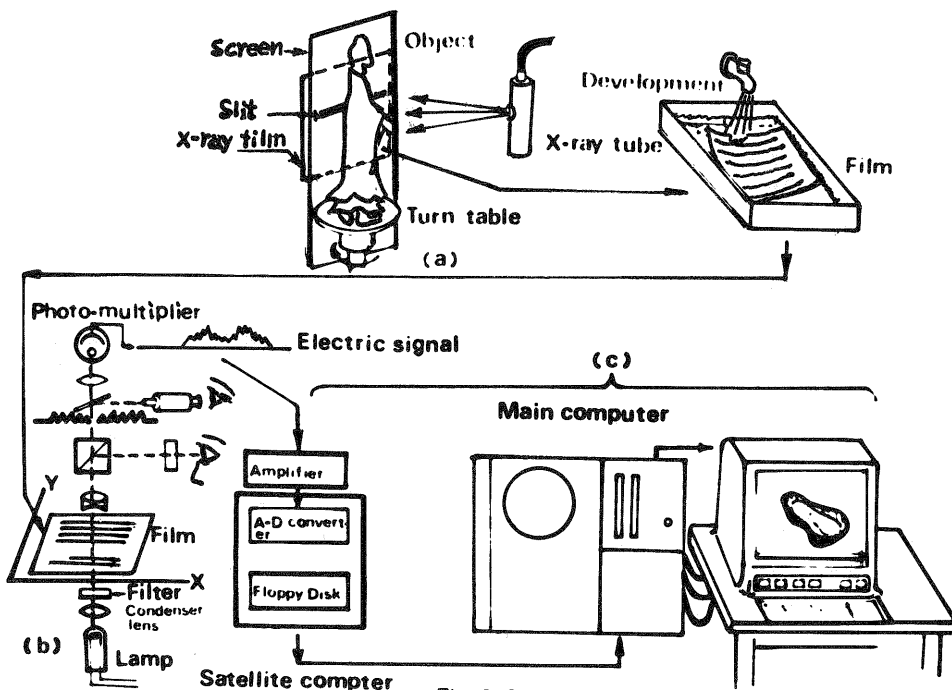


Fig. 3-2
Fig.3-2.

3-2. Parts of the instrument

(1). X-ray source

Size: 289mm X ϕ 100mm. , Weight: 8 Kg.

Angle of exposure: 40°.

Rate of cooling off: more than 4l/min. by water

Large focus: 1.5 X 1.5 mm. , 160Kvp DC(maximum tube voltage.),
10mA(tube current).

Small focus: 0.4 X 0.4 mm. , 4mA(tube current).

(2). Film shifting instrument and Turn table

The puls motor used: 2 phase, 1.8° step (refer to Fig.3-3, Fig.3-4)

(3). Film cassette

FUJI EC cassette N 35.6 X 43.2 cm

(4). Photo-pattern analyzer

OYO-DENKI KENKYUJO CO. Type : PPA-250 .

(5). Computer

Main comouter : OKITAC 50 V 15.

Satellite computer : Personal computer if 800 Model 50.

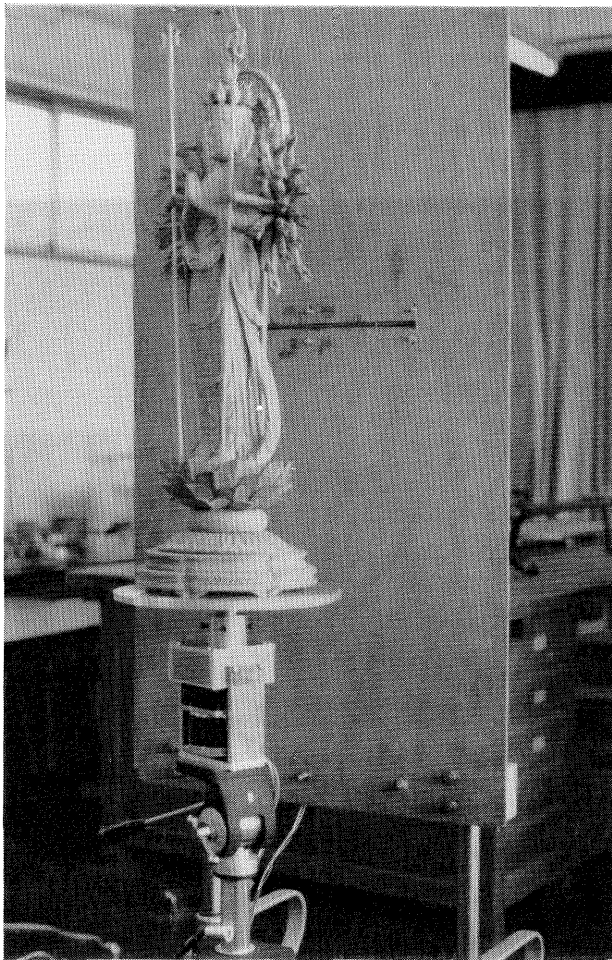


Fig. 3-3.

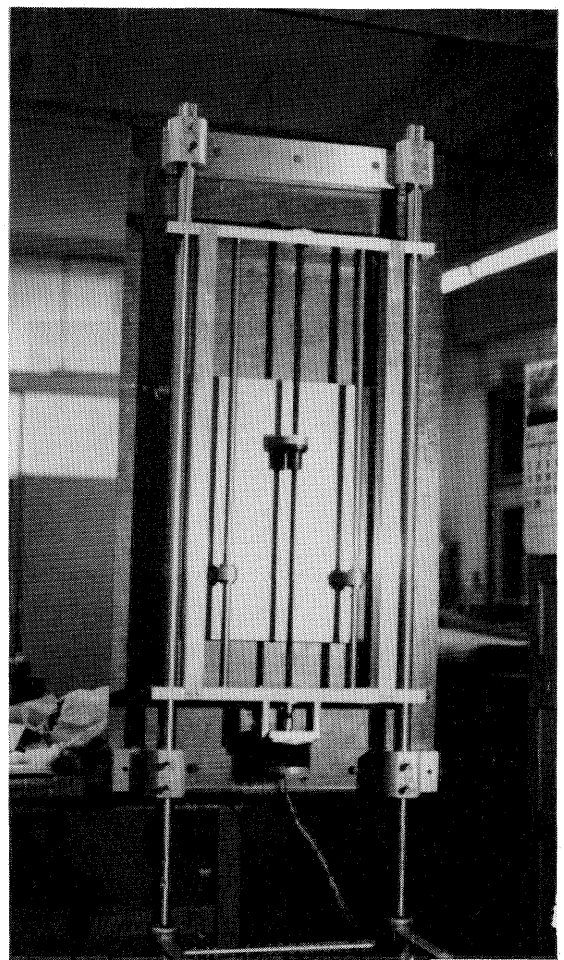


Fig.3-4.

4. Experimental example

4-1. Section of a piece of wood

A piece from a pine tree with the diameter of about 6cm was placed on a turn table as an object to collect its projected data by fan beam. Afterward, the piece was sawed and its section was photographed. Fig.4-1 and Fig.4-2 show the reconstructed tomogram and the photograph of the sawed wood section respectively.

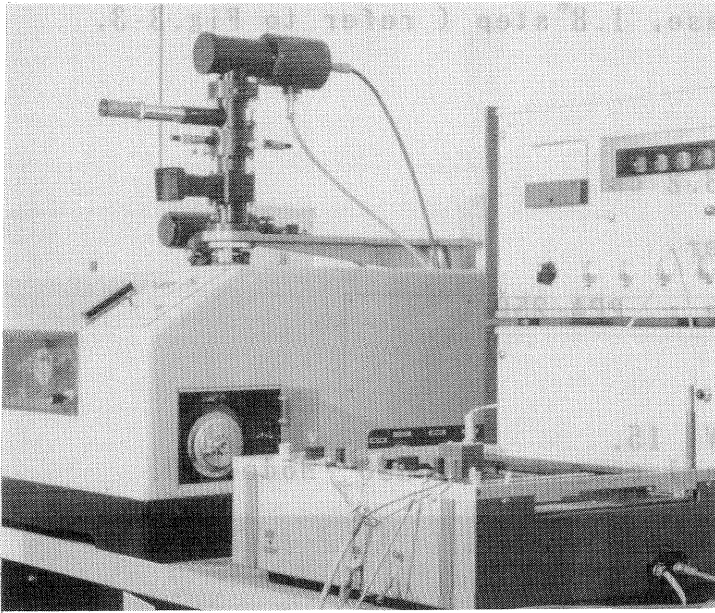


Fig.3-5.

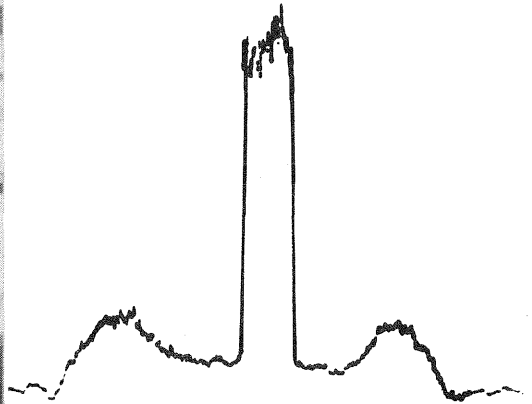


Fig.3-6

Fig.3-6.

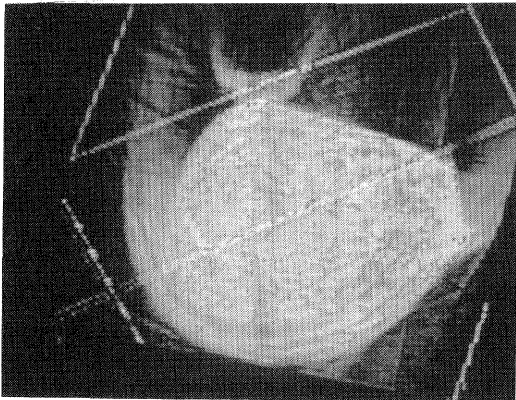


Fig.4-1.

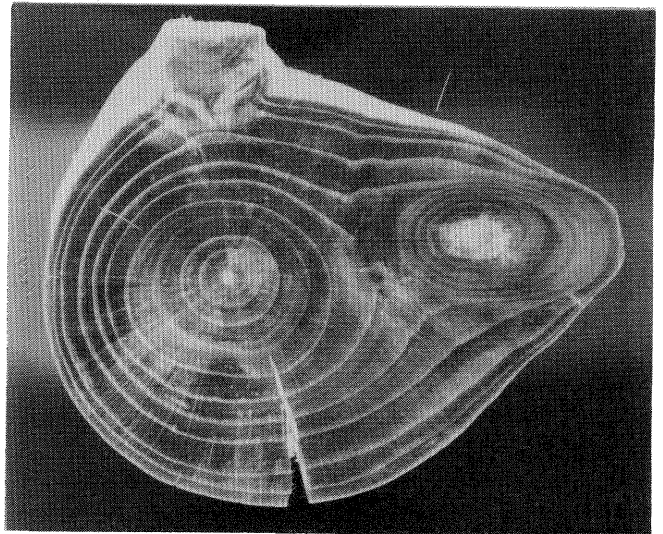


Fig.4-2.

4-2. Section of wooden SENJU KANNON (there is an iron pole inside of a wooden statue)

Fig. 4-3 : Object (SENJU KANNON).

Fig. 4-4 : Object with some control points (Here , 8 control points are seen on the object).

Fig. 4-5 : X-ray photograph of the object .

Fig. 4-6 : X-ray tomogram reconstructed in this method, which is the tomogram in the case of about 30° rotated from the front of the object.

Various simulations were performed to test the program, however, they are omitted in this report to simply propose the development of a low cost and portable CT for the purpose of the investigation of cultural property.

5. Reference

- (1) E. ORAN BRIGHAM " THE FAST FOURIER TRANSFORM "
(1974 by Prentice- Hall, Inc., Englewood Cliffs, N.J.)
(2) M. ONOE " IYO GAZO SHORI " (ASAKURA SHOTEN Co.)
(3) H. OZAKI and K. TANIGUCHI, H. OGAWA "GAZO SHORI" (KYORITSU SHUPAN Co.)



Fig.4-3.

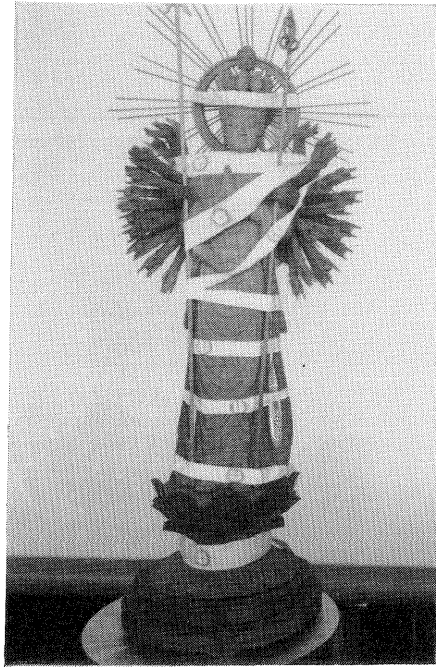


Fig.4-4.

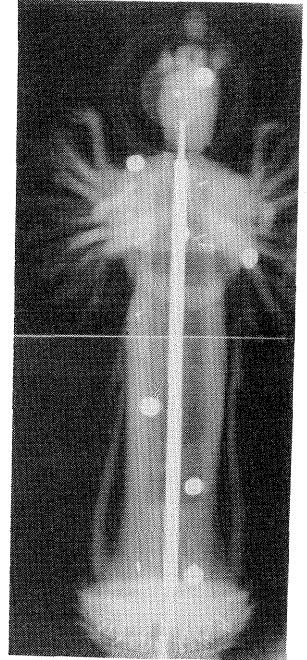


Fig.4-5.

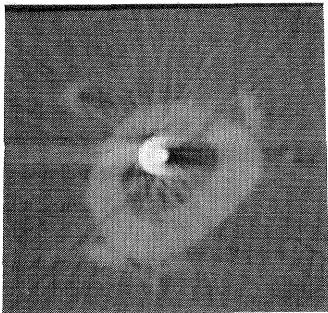


Fig.4-6.

